Linear-Scaling Linear-Response Time-Dependent Density Functional Theory in ONETEP

Nicholas D.M. Hine

Associate Professor, Theory Group, Department of Physics, University of Warwick

ONETEP Masterclass 2017

Unoccupied states and Optical Spectra

- Unoccupied states (and hence optical spectra) are not well-represented in the valence NGWF representation:

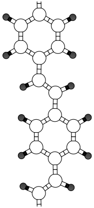

The conjugated polymer PPV - poly(para-phenylene vinylene)

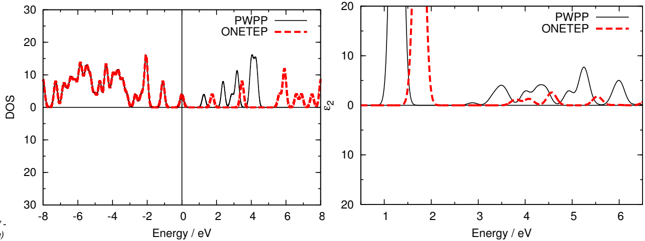

- Construct new set of NGWFs and new 'conduction state' kernel to describe ψ_c; Project out and shift valence states so that conduction states are lowermost

L. E. Ratcliff, N.D.M. Hine, P.D. Haynes, Phys. Rev. B **84**, 165131 (2012)

Unoccupied states and Optical Spectra

- Unoccupied states (and hence optical spectra) are not well-represented in the valence NGWF representation:

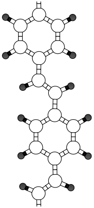

The conjugated polymer PPV - poly(para-phenylene vinylene)

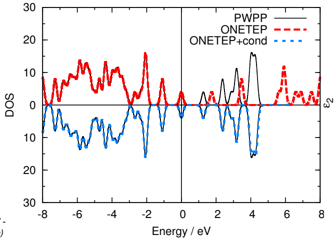

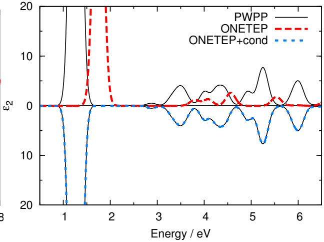

- Construct new set of NGWFs $\chi_\alpha(\mathbf{r})$ and new 'conduction state' kernel $K^{\alpha\beta}_{\{c\}}$ to describe ψ_c; Project out and shift valence states so that conduction states are lowermost
- Optimised conduction NGWFs can describe all localised states of a molecule (but not vacuum states)
- However, limitations of DFT mean bandgaps underestimated. TDDFT can improve this for small systems and localised excitations

L. E. Ratcliff, N.D.M. Hine, P.D. Haynes, Phys. Rev. B **84**, 165131 (2012)

Linear-Response TDDFT

Casida Formalism: Solve

$$\begin{pmatrix} \mathbf{A}(\omega) & \mathbf{B}(\omega) \\ -\mathbf{B}(\omega) & -\mathbf{A}(\omega) \end{pmatrix} \begin{pmatrix} \mathbf{X} \\ \mathbf{Y} \end{pmatrix} = \omega \begin{pmatrix} \mathbf{X} \\ \mathbf{Y} \end{pmatrix}$$

where

$$\begin{aligned} A_{cv,c'v'}(\omega) &= \delta_{cc'}\delta_{vv'}(\varepsilon^{\mathrm{KS}}_{c'} - \varepsilon^{\mathrm{KS}}_{v'}) + K_{cv,c'v'}(\omega) \\ B_{cv,c'v'}(\omega) &= K_{cv,v'c'}(\omega) \end{aligned}$$

and

$$K_{cv,c'v'}(\omega) = \left\langle \psi^{\mathrm{KS}}_{c}\psi^{\mathrm{KS}}_{v} \left| \frac{1}{|\mathbf{r}-\mathbf{r}'|} + f_{\mathrm{xc}}(\mathbf{r},\mathbf{r}',\omega) \right| \psi^{\mathrm{KS}}_{c'}\psi^{\mathrm{KS}}_{v'} \right\rangle$$

Tamm-Dancoff approximation: $\mathbf{Y} = 0$; $\mathbf{B} = 0$; $\mathbf{AX} = \omega\mathbf{X}$
Use iterative eigensolvers: Only the action $\mathbf{q} = \mathbf{Ax}$ is required.
ω-dependence of f_{xc} is generally dropped (eg ALDA)

LR-TDDFT with LS-DFT

Drop ω-dependence of f_{xc} for local functionals (eg ALDA)

$$\begin{pmatrix} \mathbf{A} & \mathbf{B} \\ -\mathbf{B} & -\mathbf{A} \end{pmatrix} \begin{pmatrix} \mathbf{X} \\ \mathbf{Y} \end{pmatrix} = \omega \begin{pmatrix} \mathbf{X} \\ \mathbf{Y} \end{pmatrix}$$

Make Tamm-Dancoff approximation (ignore de-excitations): $\mathbf{Y} = 0$; $\mathbf{B} = 0$; Can then use iterative eigensolvers.

$$\mathbf{A}\mathbf{X} = \omega \mathbf{X} \quad \omega = \min_{\mathbf{X}} \frac{\mathbf{X}^\dagger \mathbf{A} \mathbf{X}}{\mathbf{X}^\dagger \mathbf{X}}$$

Write $\mathbf{q} = \mathbf{A}\mathbf{X}$ via effective transition density $\rho^{\{1\}}(\mathbf{r})$ and KS eigenvalues

$$q_{cv} = (\varepsilon_c^{\mathrm{KS}} - \varepsilon_v^{\mathrm{KS}}) X_{cv} + \left(V_{\mathrm{SCF}}^{\{1\}} \left[\rho^{\{1\}} \right] \right)_{cv}$$

where $\rho^{\{1\}}(\mathbf{r}) = \sum_{cv} \psi_c^{\mathrm{KS}}(\mathbf{r}) X_{cv} \, \psi_v^{\mathrm{KS}}(\mathbf{r})$

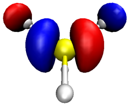

Express transition density via NGWFs & response density matrix $\mathbf{P}^{\{1\}}$

$$\rho^{\{1\}}(\mathbf{r}) = \sum_{\alpha\beta} \chi_\alpha(\mathbf{r}) P^{\{1\}\alpha\beta} \phi_\beta(\mathbf{r})$$

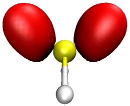

Hole / Electron each well-described by $\{\phi_\alpha(\mathbf{r})\}$ / $\{\chi_\alpha(\mathbf{r})\}$ respectively

TDDFT gradient $\mathbf{q} = \mathbf{A}\mathbf{x}$ in $\{\phi\}$ / $\{\chi\}$ representation:

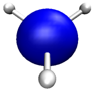

$$\mathbf{q}^{\chi\phi} = \mathbf{P}^{\{c\}} \mathbf{H}_{\mathrm{KS}}^{\chi} \mathbf{P}^{\{1\}} - \mathbf{P}^{\{1\}} \mathbf{H}_{\mathrm{KS}}^{\phi} \mathbf{P}^{\{v\}} + \mathbf{P}^{\{c\}} \mathbf{V}_{\mathrm{SCF}}^{\{1\}\chi\phi} \mathbf{P}^{\{v\}}$$

Fully $O(N)$ for each ω if $\mathbf{P}$'s truncated.

Optimise multiple $\{\mathbf{P}_i\}$ simultaneously → Scales as $O(N) \times O(N_\omega)$ with small $O(N) \times O(N_\omega^2)$ orthogonalisation step

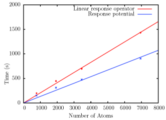

T. J. Zuehlsdorff, N. D. M. Hine, [...], P. D. Haynes , J. Chem. Phys. 139 064104 (2013).

Full TDDFT & Response Kernel Truncation

TDA often inadequate - use full TDDFT:
T. J. Zuehlsdorff, N. D. M. Hine, M. C. Payne, P. D. Haynes J. Chem. Phys. 143, 204107 (2015)

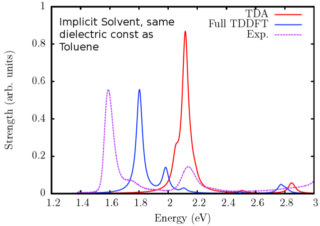

Implicit Solvent description does not correctly reproduce solvatochromic shift, use explicit solvent:

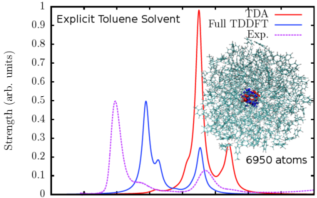

Truncation of response kernel can be used to eliminate spurious charge-transfer states

Fully dense $P^{\{1\}}$	**$P^{\{1\}}$ on Benzene A**
10th excitation:	1st excitation:
$\omega = 5.1950$ eV	$\omega = 5.1953$ eV
$f = 0.177 \times 10^{-6}$	$f = 0.111 \times 10^{-6}$
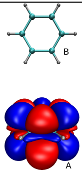	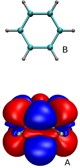

Atom-centred NGWFs provide natural means to constrain excitations to subspaces

$\Rightarrow$ significant increase in efficiency

Can reintroduce subsystem coupling perturbatively with final subspace diagonalisation: $\mathbf{P}^{\{1\}}_{\text{tot}} = \sum_I \alpha_I \mathbf{P}^{\{1\}}_{\mathbf{A}_I} + \sum_J \beta_J \mathbf{P}^{\{1\}}_{\mathbf{B}_J}$

Alizarin: Solvatochromic shifts

Alizarin prototypical red dye exhibiting strong solvatochromic shift

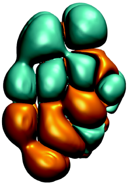
Implicit solvent

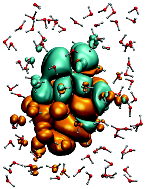
6 Å of explicit water

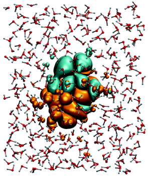
10 Å of explicit water

S_1 excitation stays mostly localised but fractions of electron and hole delocalise to water ⇒ slow convergence of solvatochromic shift

Two contributions:

- Electrostatic potential of specific configuration
- Delocalisation of transition to environment

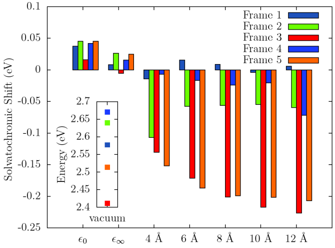

Convergence of S_1 with explicit water

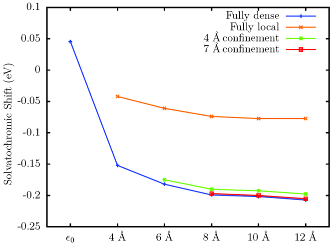

Convergence with response density matrix truncation

Quantified Natural Transition Orbital Analysis

Large systems → many low-lying excitations

How to follow excitation as geometry varies?

QNTO analysis allows adiabatic PES to be "reconnected" by matching transition origins.

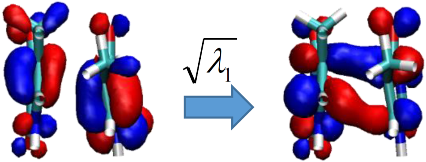

NTO1-H **NTO1-E**

Find **U**, **V** matrices that diagonalise transition density matrix.

$$\mathbf{P}_I^{\{1\}} = \bar{\mathbf{U}}_I \mathbf{D}_I \bar{\mathbf{V}}_I$$

Identify states involved in funnel resulting in thymine dimerisation

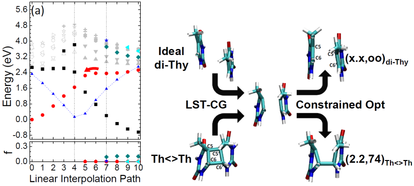

Mechanism then verified in much larger model (4 base pairs of DNA)

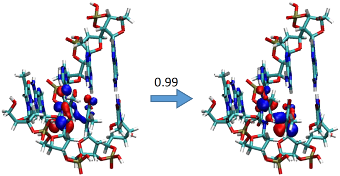

NTO1-H NTO1-E

J.-H. Li, T. J. Zuehlsdorff, M. C. Payne and N. D. M. Hine, Phys. Chem. Chem. Phys., 17, 12065 (2015)
J.-H. Li, T. J. Zuehlsdorff, M. C. Payne and N. D. M. Hine, upcoming (2015)

Colour Prediction

Nile Red (9-diethylamino-5-benzo[α]phenoxazinone)

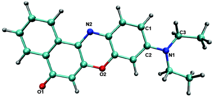

Strong solvent-dependent shift:

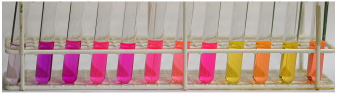

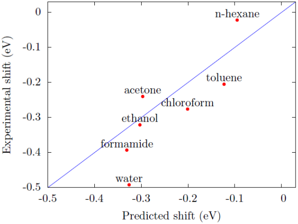

Not well-predicted by electrostatic models

Can we use the absorption spectrum to directly predict the colour?

$$I_{\text{trans}} = I_0(\lambda) e^{-\kappa(\lambda)x}$$

$\kappa(\lambda)$: absorption coefficient;
$I_0(\lambda)$: spectrum of illuminant;

$$\begin{pmatrix} X \\ Y \\ Z \end{pmatrix} = N \int I_{\text{trans}}(\lambda) \begin{pmatrix} \bar{x}(\lambda) \\ \bar{y}(\lambda) \\ \bar{z}(\lambda) \end{pmatrix} \mathrm{d}\lambda$$

$\bar{x}(\lambda)$, $\bar{y}(\lambda)$, $\bar{z}(\lambda)$: Tristimulus color matching functions

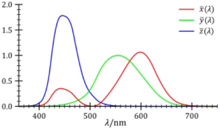

X, Y, Z can be transformed into RGB.

Nile Red Colour Prediction

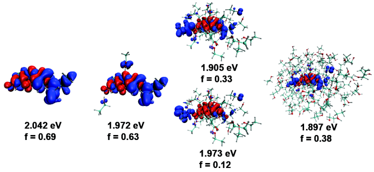

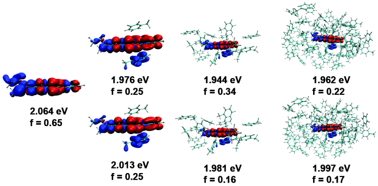

Ethanol: hydrogen bonded configurations; Toluene: $\pi - \pi$ stacked configuration.
Run long explicit solvent MD - extract samples

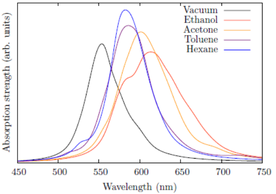

b) Implicit solvent

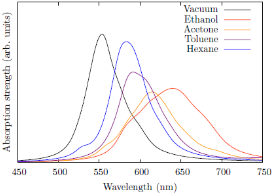

a) Explicit Solvent

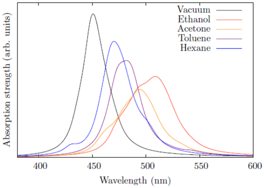

Spectral warping: calculate CAM-B3LYP spectrum, apply transformation to PBE spectrum:

$$\omega_i^{\text{trans}} = \omega_i + \beta + \alpha \phi_i^2$$

Nile Red Colour Prediction

Sufficient accuracy for useful predictive power:

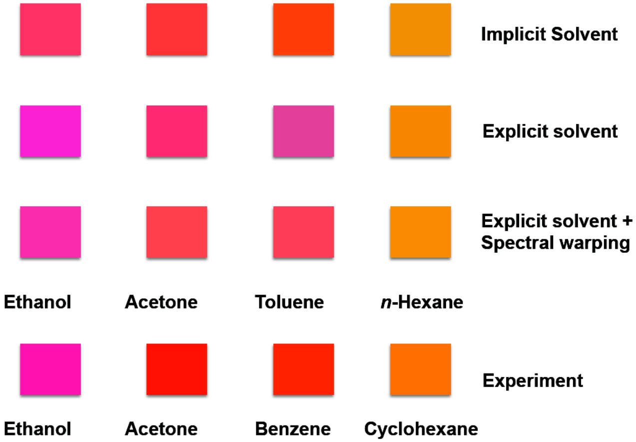

Implicit Solvent

Explicit solvent

Explicit solvent +
Spectral warping

Ethanol **Acetone** **Toluene** ***n*-Hexane**

Experiment

Ethanol **Acetone** **Benzene** **Cyclohexane**

Not yet better than colour-resolving power of the eye, but pretty good!

Energy Transport in the FMO Complex

Fenna Matthews Olson Pigment-Protein Complex: widely-studied due to evidence of quantum coherent energy transfer & near 100% photon-to-electron conversion

High-res crystal structure known via XRD

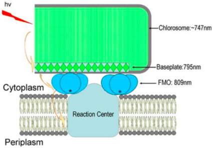

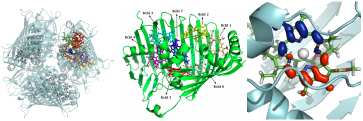

Bchl pigments held in place via non-bonded interactions with the protein.
⇒Local environment ‘tunes’ site energies. How large a system do we need to study to obtain accurate (relative) site energies?

To model electronic excitation transfer, parameterise H_{exciton}:

$$H = \sum_i \varepsilon_i |i\rangle\langle i| + \sum_{i\neq j} J_{ij} |i\rangle\langle j|$$

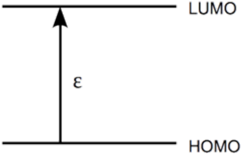

ε = “site energy”

Calculations performed first on extracted subsystems (1500 atoms) surrounding each site

Calculated Site Energies

Results very different from best QM/MM calcs with small QM regions:

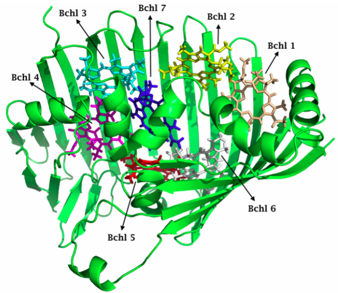

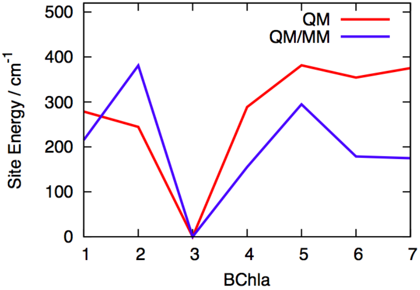

Identification of Bchl3 as the lowest energy “exit” pigment fits with alignment in membrane.

D. J. Cole, A. W. Chin, N. D. M. Hine, P. D. Haynes and M. C. Payne, J. Phys. Chem. Lett. 4, 4206 (2013).

Calculated Site Energies & Couplings

Pretty good agreement between site energies and those obtained by careful empirical fitting to experimental absorption data:

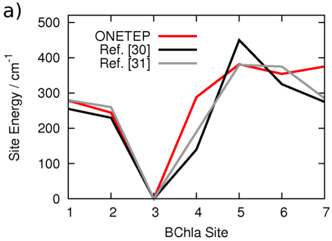

Identification of Bchl3 as the lowest energy “exit” pigment fits with alignment in membrane. Bchl4 & Bchl7 too high?

D. J. Cole, A. W. Chin, N. D. M. Hine, P. D. Haynes and M. C. Payne, J. Phys. Chem. Lett. 4, 4206 (2013).

For pigments with no orbital overlap, energy transfer is mediated by Coulombic coupling between transition densities:

$$J_{ij} = \frac{1}{\varepsilon}\int d\mathbf{r}\, \phi^{(i)}_{\mathrm{elec}}[\rho^{(i)}_{\mathrm{trans}}](\mathbf{r})\,\rho^{(j)}_{\mathrm{trans}}(\mathbf{r})$$

$$\rho^{(i)}_{\mathrm{trans}}(\mathbf{r}) = \psi^{(i)*}_{\mathrm{HOMO}}(\mathbf{r})\psi^{(i)}_{\mathrm{LUMO}}(\mathbf{r})$$

ONETEP couplings close to those from fitted classical point charge models.

NB: Empirical parameter $\varepsilon = 4$ to account for dielectric screening of protein environment

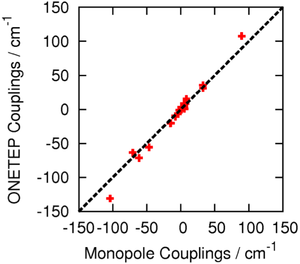

Energy Transport in FMO

Hamiltonian can be formulated *ab initio*

BChla	1	2	3	4	5	6	7
1	12444	-131	5	-7	9	-20	-11
2	-131	12410	36	8	1	15	3
3	5	36	12165	-56	0	-10	7
4	-7	8	-56	12454	-64	-20	-71
5	9	1	0	-64	12547	108	-1
6	-20	15	-10	-20	108	12519	31
7	-11	3	7	-71	-1	31	12540

Rigid shift $\Delta\omega = 3710\text{cm}^{-1}$ applied to all site energies to align with experimental spectrum

Solve dynamics: Exciton created on Bchl1 relaxes down to Bchl3 in $\sim$5ps

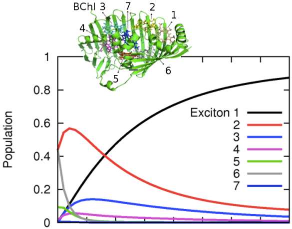

Optical Abs. & Linear / Circular Dichroism Spectra.

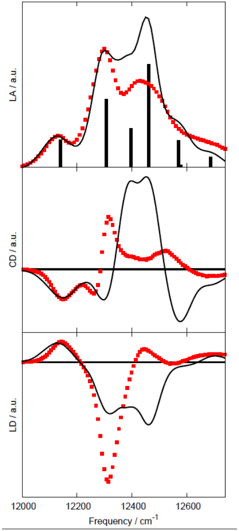

Inhomogeneous disorder by averaging over realisations with site energies individually broadened by Gaussian distribution.

Fair agreement over much of the range: near-degeneracy delocalises exciton states, boosts dipole.

Hints that description of couplings for very nearby sites may not be adequate

Can investigate effect of individual mutations on site energies to elucidate the role of the backbone: specific H-bond doners red shift by up to 130cm^{-1}

D. J. Cole, A. W. Chin, N. D. M. Hine, P. D. Haynes and M. C. Payne, J. Phys. Chem. Lett. 4, 4206 (2013).

Correlated Static Disorder in FMO

Same environment that maximises electronic coupling between pigments contains vibrational DOFs that couple to excitations
⇒Might destroy electronic coherence?

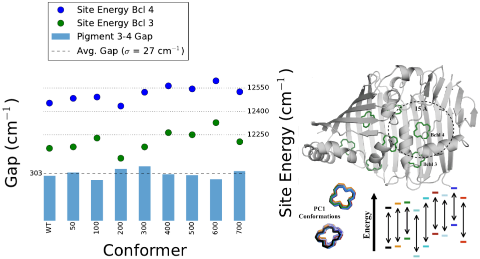

Use FIRST to identify geometric constraints and FRODA to perform constrained dynamics, identifying principal components.

Calculate site energies of conformers along PC1 using ONETEP.

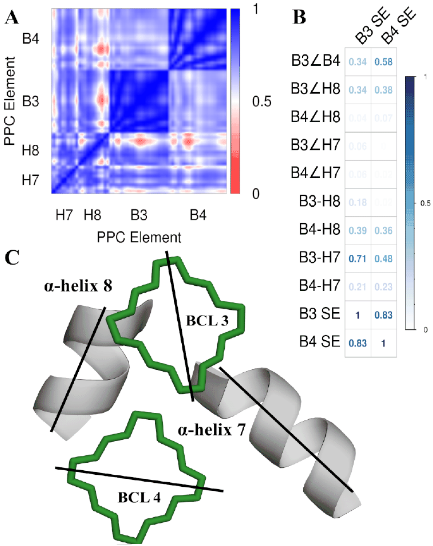

	B3 SE	B4 SE
B3∠B4	0.34	0.58
B3∠H8	0.34	0.38
B4∠H8	0.04	0.07
B3∠H7	0.06	0
B4∠H7	0.06	0.02
B3-H8	0.18	0.02
B4-H8	0.39	0.36
B3-H7	0.71	0.48
B4-H7	0.21	0.23
B3 SE	1	0.83
B4 SE	0.83	1

A. S. Fokas, D. J. Cole , N. D. M. Hine , S. Wells, M. C. Payne, and A. W. Chin, *in preparation*

Current Work: Full Monomer LR-TDDFT

Via Winton Programme "Pump Prime" grant, calculations currently underway on system comprising everything within 20 Ang of any BChl pigment in 1 FMO monomer (8990 atoms)

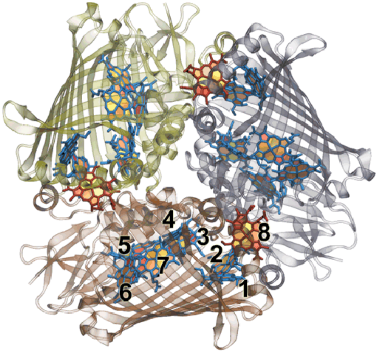

Choose sparsity pattern of $K^{\{1\}\alpha\beta}$
$\Rightarrow$ lowest excitations deloc. combo of local excitations, including coupling.

Compute unitary rotation to minimise spread to find localised basis.
$|\phi_I^{\text{site}}\rangle = U_{I\alpha}|\phi_\alpha^{\text{site}}\rangle$
$\Omega = \sum_I [\langle\phi_I^{\text{site}}|r^2|\phi_I^{\text{site}}\rangle - \langle\phi_I^{\text{site}}|r|\phi_I^{\text{site}}\rangle^2]$

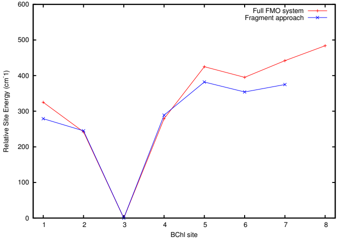

Early indications: noticeable shifts in KS-DFT, more so in TDDFT.

T. J. Zuehlsdorff, D. J. Cole, M. C. Payne, N. D. M. Hine and A. W. Chin, *in preparation*

Conclusions

- Linear Scaling DFT with ONETEP (www.onetep.org) allows DFT with plane-wave-equivalent accuracy for simulations of systems comprising hundreds to tens of thousands of atoms
- In theoretical UV/vis spectroscopy, inclusion of both an explicit representation of the environment and a high-accuracy functional are crucial to obtaining quantitative accuracy on predicted spectra.
- **Long-term vision:** simulation toolset enabling computational discovery with true predictive power for nanomaterials spectroscopy.

Acknowledgements

EPSRC
Engineering and Physical Sciences
Research Council

The Leverhulme Trust

THE WINTON PROGRAMME FOR THE
Physics of Sustainability

- Funding: EPSRC, The Leverhulme Trust (ECF), Winton Programme for the Physics of Sustainability
- Computing: Warwick CSC (Tinis), Cambridge HPC Facility (Darwin), EPCC (ARCHER), Imperial HPC Facility (CX1/CX2)
- ONETEP Developers Group (P. Haynes, A. Mostofi, C. Skylaris, M. Payne, J. Dziedzic & NDMH)

WARWICK
THE UNIVERSITY OF WARWICK

Centre for Scientific Computing

www.onetep.org